Taylor & Francis
Taylor & Francis Group

Australian Journal of Earth Sciences

An International Geoscience Journal of the Geological Society of Australia

ISSN: (Print) (Online) Journal homepage: https://www.tandfonline.com/loi/taje20

New age constraints for the Tommy Creek Domain of the Mount Isa Inlier, Australia

A. Brown, C. Spandler & T. G. Blenkinsop

To cite this article: A. Brown, C. Spandler & T. G. Blenkinsop (2023) New age constraints for the Tommy Creek Domain of the Mount Isa Inlier, Australia, Australian Journal of Earth Sciences, 70:3, 358-374, DOI: 10.1080/08120099.2023.2171124

To link to this article: https://doi.org/10.1080/08120099.2023.2171124

Published online: 05 Feb 2023.

AUSTRALIAN JOURNAL OF EARTH SCIENCES
2023, VOL. 70, NO. 3, 358–374
https://doi.org/10.1080/08120099.2023.2171124

New age constraints for the Tommy Creek Domain of the Mount Isa Inlier, Australia

A. Brown[a], C. Spandler[a,b] and T. G. Blenkinsop[c]

[a]Economic Geology Research Centre (EGRU) and Geoscience Department, James Cook University, Townsville, Australia; [b]Department of Earth Sciences, University of Adelaide, Adelaide, Australia; [c]School of Earth and Environmental Sciences, Cardiff University, Cardiff, UK

ABSTRACT
The Tommy Creek Domain is a complex, yet little studied, terrane in the Eastern Subprovince of the Mount Isa Province, northwest Queensland Australia. In this study, we take advantage of modern low-cost and rapid geochronology techniques to undertake an iterative dating approach integrated with detailed fieldwork to define the ages and extents of numerous lithologies and units of the Tommy Creek Domain. This includes some units not previously identified, lithologies previously grouped together based on field observations but now shown to have multiple distinct ages and dates not commonly represented in Mount Isan time–space plots. We identify an episode of felsic magmatism at *ca* 1640 Ma, and multimodal intrusions (*ca* 1615 Ma) immediately preceding the onset of the Isan Orogeny. A major rock package of the Tommy Creek Domain, the Milo beds, are characterised here as the youngest pre-Isan Orogeny sedimentary unit in the Eastern Subprovince (1660–1620 Ma), confirming that sedimentation and possibly rifting continued after deposition of the Soldiers Cap, Mount Albert and Kuridala groups (*ca* 1690–1650 Ma) before the onset of the Isan Orogeny (*ca* 1600 Ma). The Milo beds are thus age equivalent to the Mount Isa and McNamara groups of the Western Succession. There is evidence of a compositional shift in sedimentation coincident with the *ca* 1640 Ma Riversleigh Inversion event, previously only observed in the Western Subprovince in the Lawn Hill Platform. The application of geochronology as part of the mapping workflow can assist with differentiating geological units in terranes where field evidence is ambiguous and can aid in the focusing of objectives for field campaigns to enable the best possible interpretations to be made.

KEY POINTS

1. New ages constrain the Milo beds in the Tommy Creek Domain as the youngest stratigraphy in the Eastern Subprovince of the Mount Isa Province.
2. The Milo beds are age equivalents of the McNamara and Mount Isa groups of the Western Subprovince of the inlier.
3. Recognition of felsic and mafic intrusions with *ca* 1640 Ma and *ca* 1615 Ma ages.
4. Evidence for Riversleigh Inversion event *ca* 1640 in the Eastern Subprovince.

ARTICLE HISTORY
Received 19 October 2022
Accepted 17 January 2023

KEYWORDS
Mount Isa Inlier; Tommy Creek Domain; geochronology; Isan Orogeny; North Australian craton

Introduction

The Proterozoic Mount Isa Province is one of the most richly mineralised and geologically complex crustal blocks on Earth, and hence has been the focus of geological research for many decades. The Tommy Creek Domain (TCD) is a comparatively understudied region in the central area of the Mount Isa Province (Figure 1), despite having a number of intriguing characteristics such as: containing the youngest pre-Isan Orogeny sedimentary sequence in the Eastern Subprovince (Betts *et al.*, 2011); exhibiting higher apparent metamorphic grade than the adjacent, older blocks (Derrick, 1980a; Foster & Rubenach, 2006); and containing significant volumes of felsic and mafic volcanic rocks compared with other upper parts of the Eastern Subprovince stratigraphy. The similarities in age and sedimentary lithologies of the Milo beds—one of the major units of the TCD—and the younger units of the Western Subprovince may provide important information about the problematic links between the Eastern and Western subprovinces, as well as insights into the onset of deformation and magmatism in the Isan Orogeny.

The widespread adoption of laser ablation inductively couple mass spectrometry (LA-ICPMS) over the past decade for radiogenic isotope analysis has had a profound impact

CONTACT A. Brown alexander.brown@my.jcu.edu.au Economic Geology Research Centre (EGRU) and Geoscience Department, James Cook University, Townsville, QLD 4011, Australia
Editorial handling: Chris Fergusson

on the volume, cost and accessibility of geochronology (Harrison *et al.*, 2015; Spencer *et al.*, 2016). This has dramatically broadened the collective knowledge of age constraints across the globe but has also allowed geochronology to contribute to other aspects of Earth Science, such as geomorphological processes and paleoclimate. In this case study from the TCD, an integrated and iterative approach of detailed mapping, sample collection and geochronology analysis has yielded significant new insights into this enigmatic part of a well-studied terrane that has a robust existing geochronological framework.

Regional geology

The Mount Isa Province, located in northwestern Queensland, Australia (Figure 1), is a sequence of sedimentary, bimodal volcanic and intrusive igneous rocks (Blake, 1987) deposited and emplaced in an extensional, upper plate setting that have undergone polyphase metamorphism and contractional deformation (Betts *et al.*, 2006, 2011; Gibson *et al.*, 2018). It is also an important metallogenic province, with significant historic and current reserves of copper, gold, lead, zinc, silver and uranium in many mineralisation styles including IOCG, sediment hosted copper, shale hosted/SEDEX Pb–Zn–Ag, Broken Hill Type Ag–Pb–Zn and U–REE (Geological Survey of Queensland, 2011).

The geological framework of the Mount Isa Province has been summarised and reworked numerous times since the first major government mapping campaigns in the 1960s, 1970s and 1980s (Betts *et al.*, 2006; Blake, 1987; Blake & Stewart, 1992; Foster & Austin, 2008; Southgate *et al.*, 2000). These frameworks divide the province into both north–south-trending tectonic domains including the

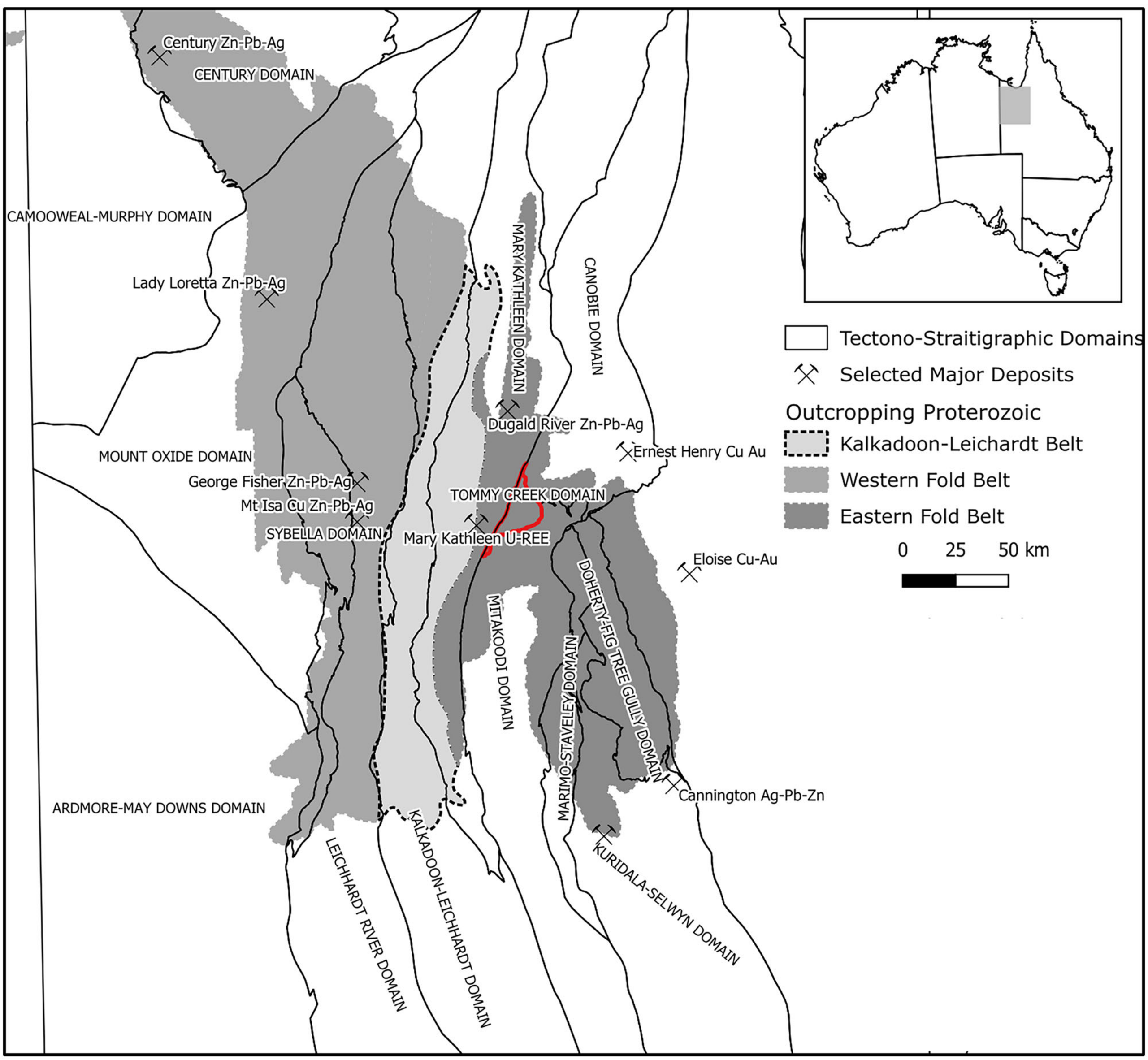

Figure 1. Overview of the Proterozoic Mount Isa Inlier. Outcropping Proterozoic basement is shaded and divided into the three main tectonic divisions. The finer tectonostratigraphic domains of Betts *et al.* (2011) are also shown, along with significant current or historic mining operations.

Western Succession/Fold Belt, Kalkadoon-Leichardt Belt and Eastern Succession/Fold Belt, and stratigraphic divisions. Two stratigraphic frameworks are used in the literature; the Cover Sequence terminology initiated by Blake (1987), and the more detailed (and Western Succession-derived) superbasin nomenclature (Southgate *et al.*, 2000).

The Blake framework divides the sedimentary and volcanic accumulations into three cover sequences. Cover Sequence 1 spans *ca* 1880–1800 Ma, Cover Sequence 2 *ca* 1800–1740 Ma and Cover Sequence 3 *ca* 1720–1575 Ma. Divisions are largely on the basis of regional scale unconformities. Further work on stratigraphic correlations and geochronology have allowed for revisions of this original framework, such as that in Foster and Austin (2008).

Detailed studies of the Western Succession resulted in the identification of the Leichardt (1800–1750 Ma), Calvert (1730–1690 Ma) and Isa (1665–1590 Ma) superbasins, and a number of sedimentary cycles and hiatuses (Jackson *et al.*, 2000; Southgate *et al.*, 2000).

Continued stratigraphic and geochronological investigations, particularly from the Geological Survey of Queensland, have led to further refinement of both the tectonic domains and stratigraphic framework (Betts *et al.*, 2011; Geological Survey of Queensland, 2011; Jell, 2013). Fifteen tectonic domains are now recognised (Figure 1) within three subprovinces; Western, Eastern and Kalkadoon-Leichardt. The stratigraphy and magmatic phases are broken into the superbasin nomenclature of Southgate *et al.* (2000) and are well summarised as time–space plots presented by Betts *et al.* (2011).

Regionally, metamorphism is dominated by high-temperature, low to medium-pressure greenschist to upper amphibolite facies assemblages, with metamorphic evolution along an anticlockwise P–T–t path (Foster & Rubenach, 2006; Hand *et al.*, 2002). Prograde metamorphic events in the Eastern Subprovince are reported at a number of ages between *ca* 1650 and 1590 (Abu Sharib & Sanislav, 2013; Giles & Nutman, 2002; Hand *et al.*, 2002; Pourteau *et al.*, 2018; Rubenach *et al.*, 2008). The thermal peak is understood to have occurred at around 1590–1575 Ma; however, this does not coincide with any regionally significant magmatic intrusions. There are numerous postulated models for producing this anomalous geothermal gradient, including compression of previously extended continental crust (Etheridge *et al.*, 1987; Oliver *et al.*, 1991); mantle delamination (Loosveld & Etheridge, 1990); heat advection via intrusions owing to high mantle heat flow (Rubenach, 1992; Rubenach & Barker, 1998; Sandiford *et al.*, 1995); radiogenic heating owing to enrichment of heat-forming elements in the upper crust (McLaren *et al.*, 1999; Sandiford *et al.*, 1998); and the burial of heat-producing stratigraphic sequences (Hand *et al.*, 2002).

Numerous tectonic syntheses have been put forward in the literature, describing multiple phases of basin development, inversion and orogeny (*e.g.* Betts *et al.*, 2006, 2011; Blake, 1987; Foster & Austin, 2008; Loosveld, 1989; Southgate *et al.*, 2000). The three cycles of dominantly east–west extensional rifting and sediment deposition represented in the superbasin stratigraphic framework are punctuated by periods of sedimentary hiatus or basin inversion, and in many places igneous intrusions (*e.g.* Burstall suite, Sybella Batholith).

The Isan Orogeny commenced *ca* 1600 Ma and continued through to *ca* 1500 Ma (Betts *et al.*, 2006), halting the superbasin development. This is the dominant period of deformation and metamorphism in the province, and can be broadly broken into four main stages; early north–south to northwest–southeast shortening (D1, 1600–1580 Ma), east–west shortening resulting in the dominant fabric of the inlier (D2, 1570–1550 Ma), reactivation and wrenching in continued east–west compression (D3, 1545–1530 Ma); and east-southeast–west-northwest direct shortening, fault reactivation and emplacement of the Williams Supersuite (1530–1500 Ma; Betts *et al.*, 2011).

The geodynamic setting of basin formation has been the subject of considerable debate. Early work suggested an intracratonic setting (Carter & Öpik, 1961), then a continental margin, based on a geochemical interpretation of the volcanic rocks (Wilson, 1978). Further geochemistry and broader scale paleogeography interpretation refuted this hypothesis (Blake, 1987; Loosveld, 1989) in favour of intracontinental rifting. A far-field margin influence forming a backarc basin in response to a southern subduction zone was put forward by workers in the early–mid 2000s (Betts *et al.*, 2006; Giles *et al.*, 2002) and is currently a favoured interpretation, although more recent work considers the associated subduction zone to have been located between the Mount Isa and Georgetown inliers, which were sutured by collision with Laurentia during the Isan Orogeny as part of the assembly of the Nuna supercontinent (Gibson *et al.*, 2018; Pourteau *et al.*, 2018).

Tommy Creek Domain

The TCD is a fault and shear bounded block covering approximately 375 km^2 in the central Eastern Fold Belt (Figures 1 and 2). It is separated from the Mary Kathleen Domain to the west by the Pilgrim-Fountain Range fault system. Unnamed structures separate TCD from the Mitakoodi Domain to the south and the Canobie Domain to east.

The dominant stratigraphic units present in the domain include the felsic volcaniclastic rocks of the Bulonga Volcanics (*ca* 1760 Ma) and the variable metasediments, marbles and calc-silicate rocks of the Corella Formation (*ca* 1740 Ma). Owing to the lack of the Mitakoodi Quartzite, this contact is a disconformity. In the central and southern parts of the TCD, the younger Milo beds (*ca* 1660–1620 Ma), which comprise volcaniclastics, metasediments, marbles, graphitic shales/schists and mafic lavas, are structurally juxtaposed against the Corella Formation.

The TCD has received relatively little attention in the literature compared with other parts of the Mount Isa Province (*e.g.* Leichardt River Domain, Mary Kathleen

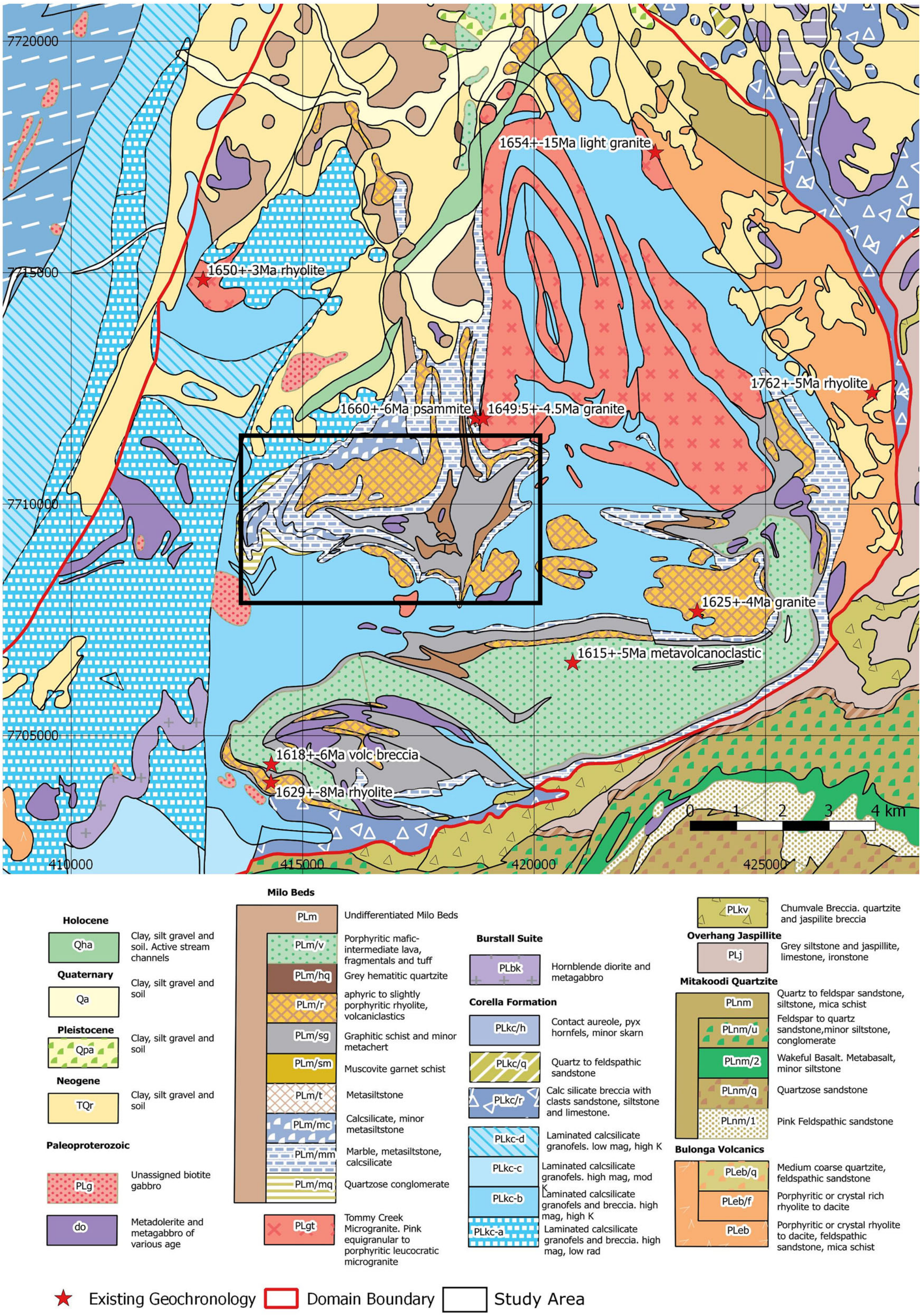

Figure 2. Geology of the central Tommy Creek Domain according to data released with the Northwest Queensland Mineral and Energy Province Report (Geological Survey of Queensland, 2011; Geological Survey of Queensland *et al.*, 2015). Geochronology sites are shown with the age and sample lithology. The black box refers to the area of Figure 3.

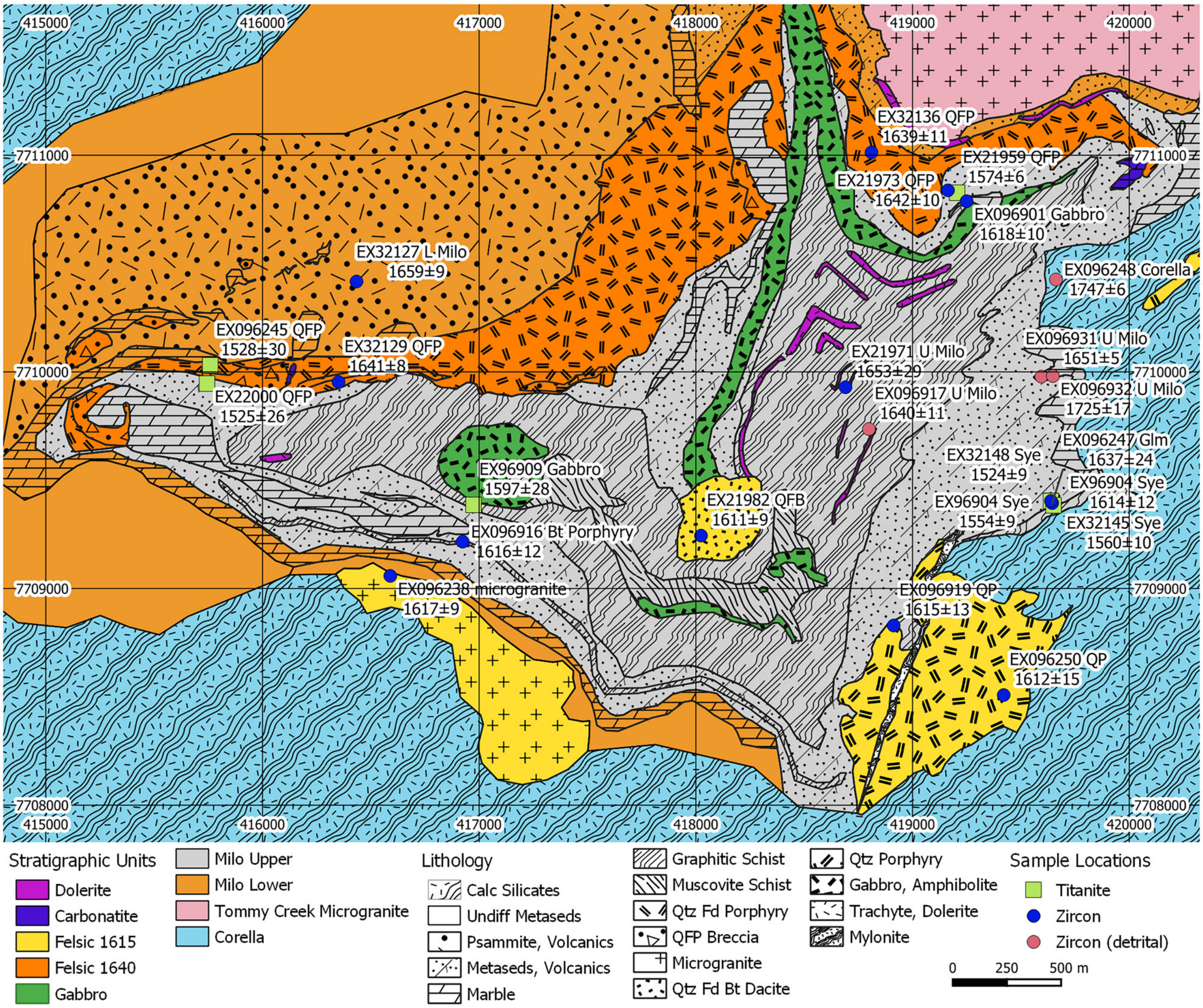

Figure 3. Sample locations with successful ages and geology of the study area. Many samples are taken from drill core and are projected to surface, and their lithology may not match the surface mapping.

Domain). The key work consists of the original government mapping (Marraba 1:100 000 sheet; Derrick, 1980b), structural mapping and geochronology by the Bureau of Mineral Resources (Hill, 1987; Hill *et al.*, 1992), and a PhD thesis (Lally, 1997). These workers identified the TCD as a fault-bounded package of calc-silicate, metasedimentary and metavolcanic rocks with felsic and mafic intrusions, and a complex and intense deformation history. The metamorphic grade is anomalously high relative to neighbouring domains, being dominated by amphibolite facies rather than the greenschist facies of adjacent blocks (Foster & Rubenach, 2006; Hill *et al.*, 1992).

The interpretation of the TCD has evolved significantly as new work was performed. The area was first mapped by the Bureau of Mineral Resources and the Geological Survey of Queensland in 1969, with revisions and first edition of the map and commentary published in 1980 (Derrick, 1980a, 1980b). In this work, the majority of the TCD is assigned to the metasedimentary Corella Formation (described as 'calcareous, dolomitic and silty beds, quartzo-feldspathic rock, limestone, basalt and black slate, and their various metamorphic variations'), intruded by the Tommy Creek Microgranite and minor mafic dykes. The commentary notes the complex cross-folding within black slates (described as andalusite and kyanite bearing) that is a feature of the central TCD (Figure 2), and the zone of amphibolite-facies metamorphism that roughly outlines the TCD.

Two samples of what was interpreted to be rhyolite within the Corella Formation were analysed by conventional zircon geochronology techniques and returned *ca* 1600 Ma ages (Page, 1983). It was recognised that these samples were strongly deformed (mylonite fabric), and shortly after, Page and Bell (1986) documented an age of 1610 ± 13 Ma for D1 deformation in the western part of the inlier. Thus, the age from the Tommy Creek rhyolites was interpreted to be that of metamorphic recrystallisation.

Targeted structural mapping of the Tommy Creek area performed in the late 1980s first recognised the 'Tommy Creek Block' as a discrete domain, bounded by the Pilgrim Fault Zone to the west, and unnamed fault and shear zones to the south and east blocks (Hill, 1987; Hill *et al.*, 1992). The Tommy Creek Microgranite was interpreted to be felsic volcanic rocks (rather than intrusive) on the basis of field relationships and rock textures. The ages of Page (1983) were refined using ion microprobe (SHRIMP) techniques on the same sample fractions as previously dated and yielded an interpreted igneous crystallisation age of 1625 ± 4 Ma. The younger original determinations were attributed to lead-loss causing averaging in bulk digestion of zircons. The volcanic and associated metasedimentary units described were therefore interpreted to represent a young sequence in comparison with the rest of the Eastern Subprovince (Hill *et al.*, 1992).

Mapping and further geochronology by Lally (1997) allowed for significant refinement of this stratigraphy. Lally recognised that the felsic volcanic rocks and porphyry on the eastern margin of the domain were much older than the previously sampled rhyolites at *ca* 1760 Ma, and likely a correlative of the Bulonga or Argylla volcanics in the Mary Kathleen and Mitakoodi domains, respectively.

Further geochronological work by Carson *et al.* (2011) reported an age of 1615 ± 5 Ma for a probable volcaniclastic rock in the Milo Basin, a 1649 ± 4.5 Ma age for a sample of Tommy Creek Microgranite, and a 1660 ± 6 Ma maximum depositional age for a psammitic unit nearby the Tommy Creek Microgranite sample (Figure 2). This culminated in a revision of the Marraba Mapsheet in 2015.

Previously published ages from the TCD are listed in Table 1. Central to the young interpretation of the Milo beds are samples of volcaniclastic rocks with ages of 1618 ± 6 Ma (Page & Sun, 1998) and 1615 ± 5 Ma (Carson *et al.*, 2011). The early conventional U–Pb ages of Page (1983) have been omitted in Table 1 in favour of the SHRIMP ages of the same samples reported in Page and Sun (1998).

Study area geology

The study area, covering approximately 13 km^2 in the central portion of the TCD, comprises a complexly folded exposure of the Milo beds juxtaposed against the surrounding Corella Formation across a faulted and sheared contact (Figure 3). The Corella Formation is dominated by granoblastic calc-silicates with variable proportions of amphibole (actinolite, hornblende), diopside, albite, orthoclase, calcite and quartz, as well as calcareous metasiltstones and lenses of calcitic marble.

The Milo beds can be separated into an upper and lower sequence, with the lower sequence comprising feldspathic psammites and volcano-sedimentary rocks with lenses of dolomitic marble. The volcano-sedimentary rocks include ribbon breccias, as well as probable relict fiamme, and correlate to the Tommy Creek Beds of Hill *et al.* (1992). The upper sequence comprises biotite metasiltstones, muscovite schist, graphitic phyllite (generally 5–15% total graphitic carbon), lenses of dolomitic marble and biotite–garnet schist. The graphitic phyllite locally contains andalusite, staurolite and sillimanite.

This metasedimentary package is intruded by a multitude of felsic, mafic and alkaline igneous rocks, of which only the Tommy Creek Microgranite has been named and described in the literature (Geological Survey of Queensland *et al.*, 2015). It is a generally pink two-feldspar equigranular leucocratic granitic rock with grainsize 1–5 mm, with local hornblende or biotite as accessory phases. This unit is predominantly found to the northeast of the study area in a doubly plunging sill complex intruding Corella Formation.

A number of rhyodacitic porphyritic igneous units have been identified as sills and stocks intruding into both the Corella Formation and Milo beds. These include quartz and feldspar phyric (QFP), quartz phyric (QP) and biotite ocelli bearing (QFB) variants. The study area is also host to alkaline intrusive phases including syenitic pegmatite and glimmerite, which form dykes up to 10 m wide that have only been identified in drill core.

Two mafic phases have been identified in the study area. The most prominent is a sill of gabbro and pyroxenite, although metamorphism has altered these rocks to a coarse amphibolite and a magnesian chlorite–pyroxene–amphibole schist, respectively, both locally garnet bearing. Relict olivine has been observed in the chlorite schist. The second phase is a fine- to medium-grained biotite bearing dolerite to trachyte. Both are found as dykes or sills

Table 1. Summary of geochronology results from the Tommy Creek Domain. SHRIMP data from Geoscience Australia (Anderson *et al.*, 2017).

Lithology	Unit	Method	Age (Ma)	Error (Ma)	Age type	Publication
Rhyolite	Bulonga Volcanics	SHRIMP	1762	5	Crystallisation	
Psammite	Milo beds	SHRIMP	1660	6	Max dep	
Rhyolite	Tommy Creek Microgranite	SHRIMP	1650	3	Crystallisation	
Pink microgranite	Tommy Creek Microgranite	SHRIMP	1649.5	4.5	Crystallisation	
Rhyolite	'Tommy Creek Beds'	SHRIMP	1629	8	Crystallisation	(Page & Sun, 1998)
Microgranite	'Tommy Creek Beds'	SHRIMP	1625	4	Crystallisation	(Hill *et al.*, 1992; Page & Sun, 1998)
Brecciated volcanic	'Tommy Creek Beds'	SHRIMP	1618	6	Max dep	(Page & Sun, 1998)
Meta volcanoclastic	Milo beds	SHRIMP	1615	5	Max dep (unimodal)	(Carson *et al.*, 2011)
Garnet–staurolite schist	Milo beds	Sm–Nd garnet	1585		Prograde metamorphism	(Hand *et al.*, 2002)
Garnet–staurolite schist	Milo beds	Sm–Nd garnet	1575		Prograde metamorphism	(Hand *et al.*, 2002)

The Sm–Nd garnet ages are from an abstract (Hand *et al.*, 2002), so further details are unavailable.

primarily in the upper Milo beds, with the metagabbro–pyroxenite true thickness likely exceeding 100 m.

Deformation at the map scale is apparent as an early east–west fold subsequently refolded in a north–south orientation (Figure 2). Strong foliations and crenulation cleavages manifest in micaceous lithologies of the upper Milo beds, and the rhyodacite porphyries exhibit strong linear fabrics. Metamorphic assemblages, particularly the sillimanite in the graphitic phyllite, point towards peak thermal conditions of >500 °C, as reported by previous workers (Foster & Rubenach, 2006; Hand *et al.*, 2002).

Methods

Mapping, surface and drill-core sampling was conducted over a number of field campaigns, with the results helping to inform subsequent sampling priorities and remapping. Target minerals zircon and titanite were collected from samples via heavy mineral separation techniques and mounted in epoxy resin pucks prior to polishing. Mounts were analysed using a Hitachi SU5000 for both backscattered electron (BSE) and cathodoluminescence (CL) imaging for grain screening and spot analysis location selection. Spot analyses were performed using a Teledyne Analyte G2 193 nm ArF Excimer Laser Ablation system with a HeLex II sample cell, and a Thermo iCAP-RQ quadrupole mass spectrometer. Ablation was performed at 5 Hz and 2.5–3 J/cm^2, with spot sizes varying with target species and grainsize between 20 μm and 50 μm. Full instrument conditions are outlined in Todd *et al.* (2019).

For zircon, calibration standard GJ1 was used (Jackson *et al.*, 2004), with FC1, Temora and 91500 used as secondary check standards (Black *et al.*, 2003; Paces & Miller, 1993; Wiedenbeck *et al.*, 1995). Titanite standard MKED1 was used for calibration, with KHAN as check standard (Spandler *et al.*, 2016). All analyses were carried out at the Advanced Analytical Centre, James Cook University, Townsville. Data reduction was performed using the Iolite software package (Paton *et al.*, 2011), and final processing utilised Isoplot v. 4.15 (Ludwig, 2012). Detailed methodology, QAQC and processing notes are available in the data repository.

Results

A total of 23 ages were determined for samples across nine units, taken from the central region of the TCD. The samples yielded a variety of distributions of analyses with examples given in Figure 4; including concordant analyses (Figure 4d), concordant groups with tails of discordant results indicating Pb loss trends (Figure 4b, c, e, f) and detrital populations (Figure 4a). Ages reported here are Tera Wasserberg intercept ages unless otherwise noted.

Sample locations are shown in Figure 3, and results are represented in the context of the study area stratigraphy schematically in Figure 5. It should be noted that many samples are from drill core, and thus the given rock type does not always correlate with the surface geology. Detailed results and concordia plots for all samples are included in the data repository.

Zircon U/Pb dates from volcanic and metasedimentary rocks

Zircon dates were collected from five samples of metavolcanic and metasedimentary rocks of both the Corella Formation and Milo beds (Table 2).

One sample of albite-rich banded calc-silicate of the Corella Formation (EX096248) was taken from drill core and yielded a high number of zircons. The 63 spot analyses show a relatively clear spectrum of results, as would be expected for a detrital population (Figure 4a). A large proportion of the data are discordant; however, inspection of their distribution indicates three arrays are present, with a few outliers. Two of these arrays plot at 2572 ± 110 Ma and 1891 ± 47 Ma, along with a few near concordant outliers >3000 Ma. These likely represent pre-Barramundi basement sources (Betts *et al.*, 2011). The most numerous and concordant array yields a Tera Wasserberg age of 1756 ± 10 Ma and a Pb–Pb weighted average (concordant samples only) of 1747 ± 6 Ma. For this sample, this is considered the maximum depositional age.

Extracting zircons from various rocks of plausible volcanic origin from the Milo beds was problematic, despite many samples returning whole-rock assays of 500 ppm Zr or greater. Closer inspection of these samples, thought to represent tuffs or similar volcanic rocks, showed a high abundance of rutile and other titanium minerals, which are likely reservoirs for some Zr. Additionally, SEM imaging indicated extremely small (<10 μm) zircon inclusions present in other minerals. Only two samples of volcanic or clastic origin yielded good data.

EX32127, a feldspathic rock interpreted as a fine felsic volcanic rock towards the base of the Milo beds, produced an age of 1659 ± 10 Ma from mostly concordant analyses with minor Pb loss (Figure 4b). Although interpreted as a volcaniclastic rock, it is not clear that this represents the age of crystallisation, and it is thus considered a maximum depositional age. This age is consistent (1660 ± 6 Ma) with GSQ/GA sample 19256950 (Anderson *et al.*, 2017), also taken in the very lowest part of the sequence.

EX096917 is a sandy muscovite schist taken from near the top of the exposed Milo beds in the study area and forms an interlayer in the dominantly graphitic part of the stratigraphy. A main population of concordant and discordant analyses yields an age of 1640 ± 11 Ma, with some near concordant outliers present around 2400 and 1800 Ma. The age is best interpreted as a maximum depositional age, although if this material were dominantly volcanic in origin, it might represent the age of deposition. The lack of substantial additional populations, and coherent U/Th ratio, suggests the zircons are mostly from a single source. This age overlaps with that of the Quartz–Feldspar Porphyry

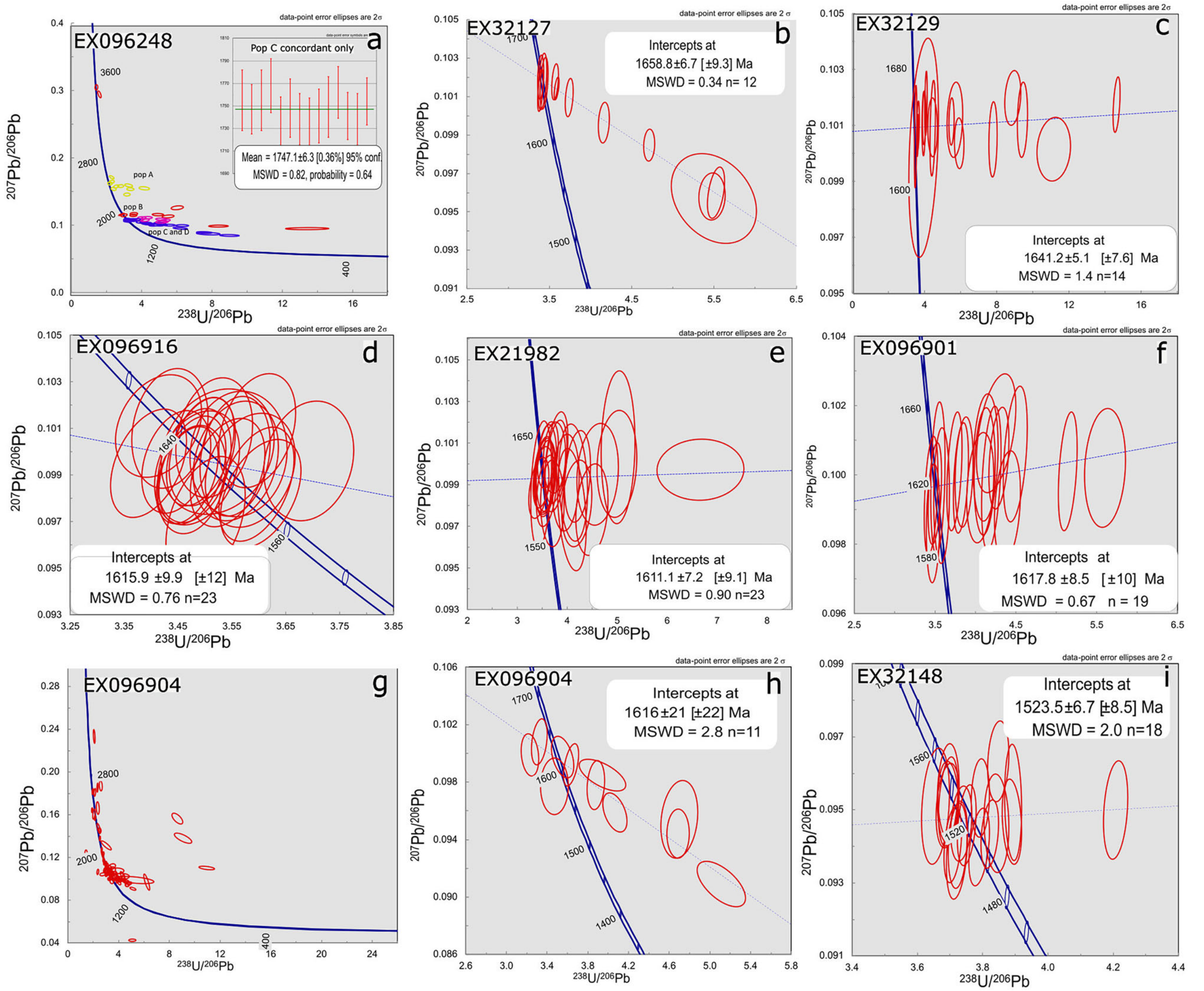

Figure 4. Selected Concordia diagrams from eight zircon or titanite samples from this study. (a) EX096248—Corella Formation metasediment showing multiple detrital zircon populations. Concordant members of population C were used to calculate the Pb–Pb age of 1747 ± 6 Ma. (b) EX32127—concordant–discordant array of the dominant population from a massive felsic rock. Interpreted as a maximum depositional age but may be crystallisation age. (c) EX32129—concordant–discordant single population from QFP unit (Quartz Feldspar Porphyry). (d) EX096916—concordant single population from a thin dark porphyritic rock intruding the Milo beds, thought to be equivalent to GA sample 1980491 (Carson *et al.*, 2011). (e) EX21982—concordant–discordant single population from biotite-bearing rhyodacite (QFB) stock that intrudes the upper Milo beds and metagabbro sills. (f) EX096901—concordant–discordant single population from fine-grained mafic dyke cutting through coarse metagabbro. (g) EX096904—zircon results showing a high degree of scatter and discordance typical of those from the syenitic pegmatites, and also glimmerite. (h) Possible coherent population; confidence in what this age represents is low. (i) EX32148—mostly concordant single population from a single large titanite crystal in syenitic pegmatite (same source as EX096904).

(QFP), which intrudes the middle part of the Milo beds, pointing towards intrusion (and associated extrusive counterparts) contemporaneous with deposition.

In addition to felsic and clastic rocks, a number of samples from carbonate rocks successfully yielded ages. Two (EX096931, EX096932) are interpreted to be metasedimentary from field relations and produced detrital populations. The ages represented in these samples of *ca* 1650 Ma, *ca* 1725 Ma and 2700–1850 Ma are consistent with the clastic Milo beds samples and other major zircon sources for the Eastern Succession. As such, a maximum depositional age of 1652 ± 5 Ma is indicated for these rocks.

These ages also confirm a significant age gap of *ca* 90 Ma and disconformity/structural contact between the Corella Formation (*ca* 1750 Ma maximum depositional age) and the Milo beds (*ca* 1660 Ma maximum depositional age).

Zircon U/Pb dates from intrusive rocks

Eleven samples of eight different intrusive igneous units are presented in Table 3. Three samples were taken from the prominent QFP unit, which forms a folded sill intruding into the transition between the upper and lower Milo beds. The three samples yielded good ages within error of each other at *ca* 1641 Ma. This coherent age group is distinct from the second group of felsic samples dated both in age and in subtle compositional and textural characteristics.

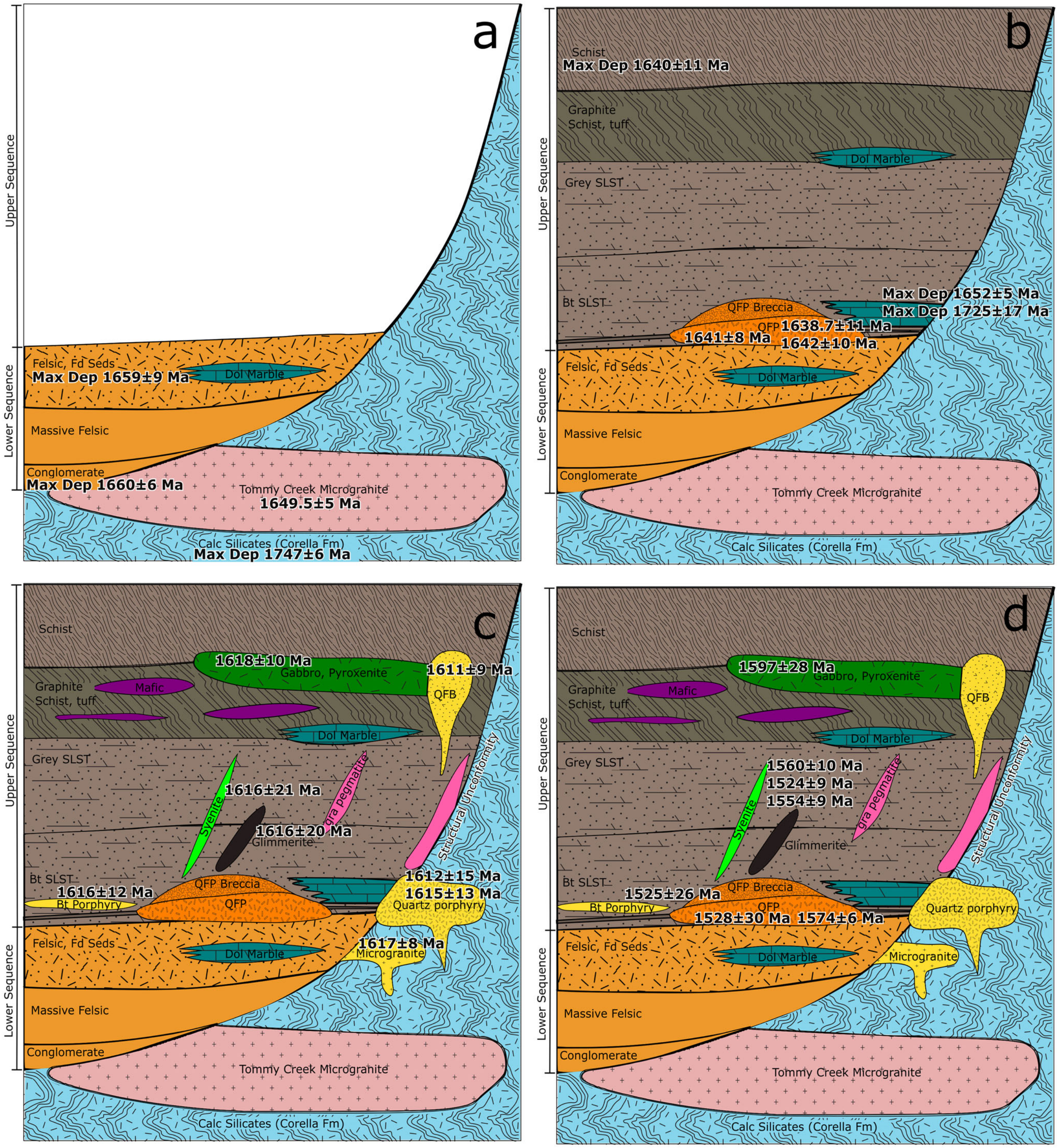

Figure 5. Schematic stratigraphy of the study area broken into four age ranges based on published ages and those presented in this paper. Disconformity between the Milo beds and Corella Formation is a fault boundary, and unit relationships represent observed field relationships. True thickness of units is poorly understood and is not to scale. (a) 1650 Ma—Corella Formation 'basement' with Tommy Creek Microgranite, and lower Milo beds; (b)1650–1630 Ma—upper Milo beds deposition and intrusion of Quartz–Feldspar Porphyry (QFP) sills; (c) 1630–1610 Ma—polymodal intrusions; and (d) post 1600 Ma—Titanite alteration events.

Five felsic samples have consistent ages of *ca* 1615 Ma, which is distinct from that of the QFP unit. However, this group is more compositionally diverse, including quartz-dominated porphyry, a darker biotite-rich stratiform porphyry, a two-feldspar microgranite and a fine quartz–feldspar biotite rock with biotite ocelli. All of these except the dark porphyry form as stocks intruding into Corella Formation calc-silicates proximal to the disconformity, or the Milo beds. The dark porphyry (EX096916) was sampled from a thin stratiform horizon towards the base of the graphite-rich upper Milo beds.

Table 2. U–Pb zircon ages from volcanic and metasedimentary rocks.

Sample	Lithology	Unit	Spots	Age 1 (Ma)	Age 2 (Ma)	Comment
EX096248	Albite calc-silicate	Corella Formation	63 (20 μm)	1747 ± 6 (*n* = 14)		Pb–Pb max depositional age
EX32127	Medium- to fine-grained felsic rock	Lower Milo beds	24 (30 μm)	1659 ± 9 (*n* = 12)		Max depositional age
EX096917	Muscovite schist, graphitic sequence	Upper Milo beds	55 (30 μm)	1640 ± 11 (*n* = 39)		Max depositional age. One main population, some outliers/singletons
EX096931	Biotite marble with shale interbeds	Upper Milo beds	60 (30 μm)	1652 ± 5 (*n* = 36)	1720 ± 21 (*n* = 12)	Pb–Pb max depositional age. Concordant singletons 2600–1850
EX096932	Biotite marble	Upper Milo beds	47 (30 μm)	1725 ± 17 (*n* = 9)	2700–1850	Pb–Pb max dep on concordant results

Table 3. U–Pb zircon ages from intrusive igneous rocks.

Sample	Lithology	Unit	Spots (size)	Age (Ma)	Comment
EX21973	Feldspar porphyry	QFP	24 (30 μm)	1642 ± 10 (*n* = 24)	Crystallisation age
EX32129	Quartz–feldspar porphyry, foliated, minor muscovite	QFP	24 (30 μm)	1641 ± 8 (*n* = 24)	Crystallisation age
EX32136	Quartz–feldspar porphyry	QFP	28 (30 μm)	1639 ± 11 (*n* = 28)	Crystallisation age
EX096901	Fine-grained mafic within coarse metagabbro	Metagabbro	19 (30 μm)	1618 ± 10 (*n* = 19)	Crystallisation age
EX096238	Pink microgranite		23 (30 μm)	1617 ± 9 (*n* = 23)	Crystallisation age
EX096916	Narrow dark porphyritic rock below graphitic schist		31 (30 μm)	1616 ± 12 (*n* = 31)	Crystallisation age
EX096919	Porphyritic schist with strong lineation	QP	48 (30 μm)	1615 ± 13 (*n* = 22)	Crystallisation age. Long Pb loss trend
EX096250	Medium coarse quartz porphyry	QP	30 (40 μm)	1612 ± 15 (*n* = 30)	Crystallisation age
EX96904	Very coarse pegmatitic syenite. Amph–fd–bt–tit. Some late qtz	Syenite pegmatite	94 (30 μm)	1616 ± 21 (*n* = 11)	Very scattered data, possible common Pb
EX096247	Coarse phlogopite– K-feldspar	Glimmerite	32 (20 μm)	1616 ± 20 (*n* = 11)	Scattered data, difficult to identify populations
EX21982	Fine quartz–feldspar with biotite ocelli to 20 mm	QFB	25 (20 μm)	1611 ± 9 (*n* = 25)	Crystallisation age

Numerous attempts were made to extract zircons from the various mafic units in the study area, including some exceptionally Zr rich samples (>500 ppm Zr). Only one sample (EX096901) yielded zircons during mineral separation, a small fine-grained mafic dyke cutting through the coarse-grained gabbro unit. This sample yielded a reasonably robust age of 1618 ± 10 Ma (Figure 4f), placing it as contemporaneous with the late felsic intrusions. Given the mafic composition, it is plausible that these zircons are xenocrystic; however, considering the uniformity of the concordant results, the zircon morphology (low aspect ratio) compared with potential sources (generally high aspect ratio) and that the sample is a late stage within the metagabbro intrusion, a syn magmatic interpretation is favoured (Bea *et al.*, 2022). The samples of alkaline rocks (glimmerite, syenitic pegmatite) yield quite poor data that are difficult to interpret. Both the syenite and glimmerite have populations indicative of *ca* 1616 Ma and include older populations that are perhaps inherited zircons.

U/Pb titanite dates

Seven samples of titanite from alteration (*e.g.* vein) and of metamorphic origin yielded good dates and are presented in Table 4, with textures illustrated in Figure 6. Analyses for samples form populations that are both concordant and discordant (*e.g.* Figure 4i), but they do not show clear evidence for multiple populations. Analyses generally show very low to absent common lead, which is commonly seen in hydrothermal titanites from the Mount Isa Province (Spandler *et al.*, 2016). For samples where common lead trends are apparent, the upper $^{206}Pb/^{207}Pb$ intercept is broadly consistent with the common lead composition of Stacey and Kramers (1975). In these cases, the lower concordia intercept is interpreted as the titanite crystallisation age.

Two samples of the fine pervasive titanite alteration that appears proximal to carbonatite veins (EX096245, EX22000; Figure 6b, d) returned consistent ages of *ca* 1525 Ma. The single grain sample from an amphibole–scapolite–calcite vein (EX21959; Figure 6c) cutting QFP returned an older age of 1575 ± 6 Ma.

Samples EX32145 (1560 ± 10 Ma) and EX32148 (1524 ± 9 Ma) have exceptionally large crystals of titanite (>15 mm) within a syenitic pegmatite (Figure 6a). The analyses do not indicate there is any distinct age zonation within the crystals; however, the ages of the two crystals are distinctly different. Sample EX96904 is a bulk rock sample from drill core, which includes EX32148 (although none of the specific crystals would have been present). Thus, it is interesting that there was no evidence for the EX32148 age within the data for EX096904, which formed a reasonably tight concordant–discordant array around 1554 ± 9 Ma and is within error of the single crystal age of EX32145. Both sets of ages are considerably younger than the ages

Table 4. U–Pb dates from titanite.

Sample	Lithology	Unit	Spots (size)	Age (Ma)	Comment
EX096909	Coarse metagabbro	Metagabbro	24 (50 μm)	1597 ± 28 (*n* = 24)	Multiple grains. Discordant
EX21959	Large crystal in vein in QFP	QFP	20 (50 μm)	1574 ± 6 (*n* = 20)	Single crystal. Most concordant
EX096245	Pervasive alteration of QFP	QFP	16 (30 μm)	1528 ± 30 (*n* = 15)	Multiple grains. Discordant. 30 μm
EX22000	Pervasive alteration of QFP	QFP	20 (50 μm)	1525 ± 26 (*n* = 15)	Multiple grains. Discordant
EX32145	Coarse amph–K-spar–bio pegmatite	Syenite	20 (50 μm)	1560 ± 10 (*n* = 14)	Single grain. Most concordant
EX096904	Coarse amph–K-spar–bio pegmatite	Syenite	17 (50 μm)	1554 ± 9 (*n* = 17)	Multiple grains (interval includes EX32148). Concordant
EX32148	Coarse amph–K-spar–bio pegmatite	Syenite	20 (50 μm)	1524 ± 9 (*n* = 18)	Single grain. Most concordant

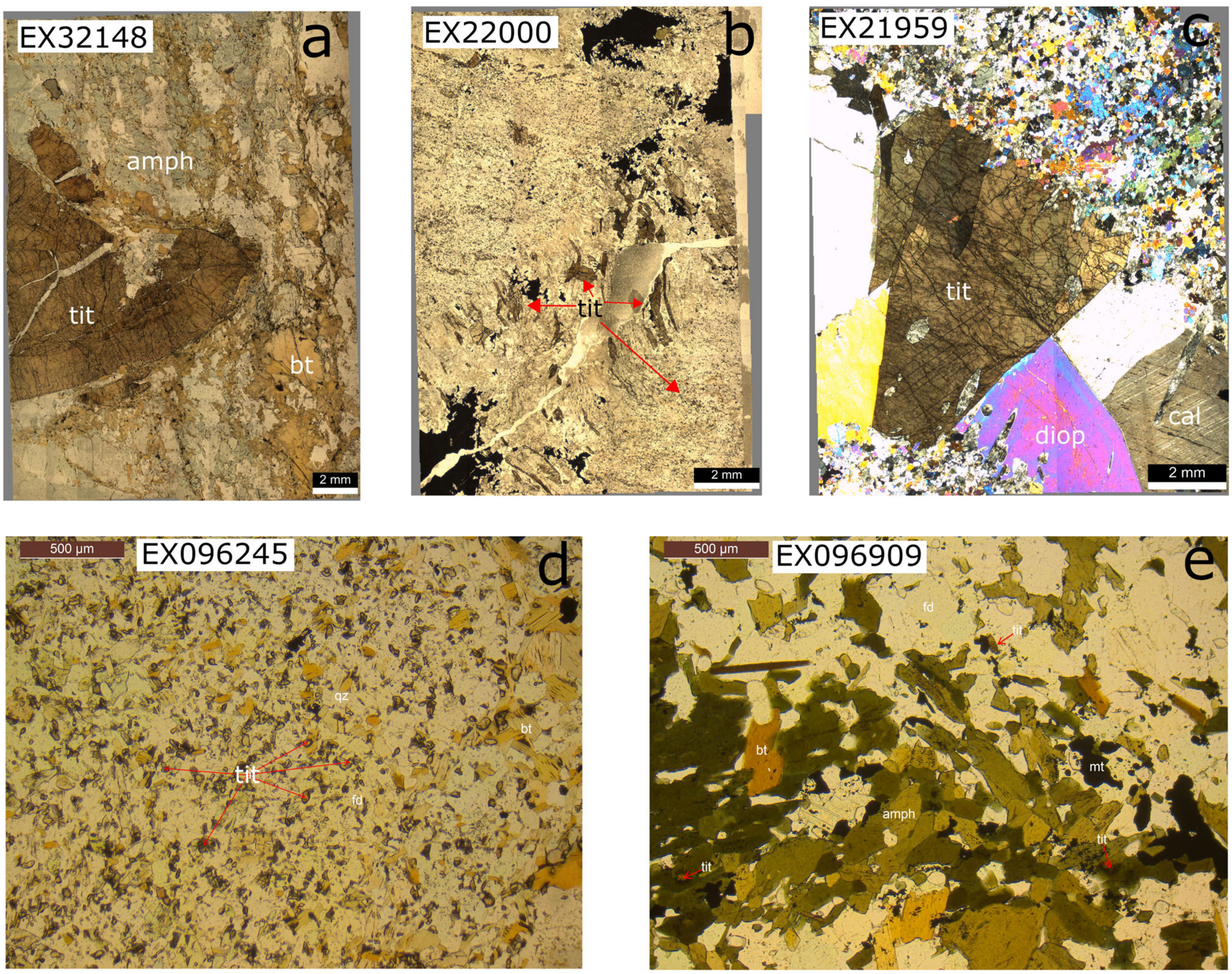

Figure 6. Photomicrographs illustrating various titanite textures of the analysed samples: (a) EX32148, a megacrystic (>1 cm) titanite within a syenitic pegmatite, plane-polarised light (PPL); (b) EX22000, vein and pervasive titanite alteration through Quartz–Feldspar Porphyry (QFP), PPL; (c) EX21959, diopside–calcite vein with large (~1 cm) titanite grain cutting through altered QFP, cross polarised light; (d) EX096245, pervasive fine titanite–biotite alteration in QFP, PPL; and (e) EX096909, metagabbro bearing fine titanite, likely as reaction products of original titanomagnetite, pyroxenes and/or amphiboles, PPL.

indicated from zircon, but the zircon data are scattered and imprecise (1616 ± 21 Ma; Figure 4g). The titanite ages are interpreted to represent ages of metamorphism or hydrothermal alteration, particularly as indicated peak thermal conditions for the area approach the U–Pb closure temperature for titanite ~600 °C (Cherniak, 1993; Frost *et al.*, 2001).

Analyses in the gabbro sample EX096909 (Figure 6e) show a common lead trend without any concordant analyses, but still form a reasonable array that intersects concordia at 1597 ± 28 Ma.

Discussion

Chronostratigraphic framework of the Tommy Creek Domain

The interpretation of stratigraphy and lithologies present in the TCD has evolved each time new geochronology data have been presented. The data in this study build substantially on the previous work, with additional units identified largely owing to the new ages. This allows for more detailed interpretation and expansion of the previously published frameworks (Betts *et al.*, 2011; Hill *et al.*, 1992).

The oldest units present in the TCD are found on the eastern margin as a wedge of metavolcanics and metasediments of the Bulonga Volcanics at 1762 Ma (Anderson *et al.*, 2017), followed by the *ca* 1740 Ma Corella Formation (Betts *et al.*, 2011). The calc-silicate metasediments of the study area are most likely from the Corella Formation, with sample EX096248 showing a maximum depositional age of 1747 ± 6 Ma.

The earliest intrusive activity is recorded in the largest and most prominent intrusive feature of the TCD, the doubly plunging sill complex of the Tommy Creek Microgranite intruding the Corella Formation, with an age of *ca* 1650 Ma (Anderson *et al.*, 2017). This closely followed deposition of volcaniclastic rocks at the base of the Milo beds at *ca* 1660 Ma, from this study and previous workers (Figure 5a; Anderson *et al.*, 2017).

The QFP sills represent a further pulse of intrusive activity at *ca* 1641 Ma; an age that is similar to the maximum deposition age of the higher parts of the Milo beds (EX96917; this study). While no field textures indicative of synsedimentary intrusion have been observed, it is plausible that these intrusions represent subsurface elements of magmatism contributing to the sedimentary pile that they intrude. The *ca* 1641 Ma QFP intrusions have only been observed within the Milo beds (Figure 5b).

Between 1620 and 1610 Ma, additional stocks and stratiform sills of variable composition, including quartz porphyry, biotite-rich rhyodacite and microgranite intruded into both the Milo beds and the Corella Formation, including along the now structural disconformity between them (Figure 5c). Initial field interpretations did not differentiate between the QP and the QFP units, although the ages clearly demonstrate they are different phases.

This 1620–1610 Ma period included mafic activity and probably also the alkaline dykes. This may point towards a burst of tectonic activity preceding or during the early stages of the Isan Orogeny. The most prominent unit, a metagabbro–pyroxenite sill, produced a titanite age (likely metamorphic) of 1597 ± 28 Ma as a lower limit to the possible intrusion age, although this age is relatively imprecise. A better constraint for the metagabbro comes from a small crosscutting fine-grained dyke (EX96901), with a robust age of 1618 ± 10 Ma. Additionally, map patterns indicate the sill is also intruded by a 1611 ± 9 Ma felsic stock (QFB, EX21982; Figure 5c).

An upper limit for the age of the sill is the 1660 Ma maximum depositional age of the lower Milo beds. No direct interaction between the metagabbro and QFP has been observed, with the metagabbro intruding at a slightly higher level in the stratigraphy. Thus, the 1641 Ma age of the QFP cannot be used to robustly constrain the mafic intrusion age. The metagabbro intrudes into the lower graphitic part of the upper Milo package, and sample EX096917 indicates these rocks to be younger than 1640 Ma, providing a likely upper limit on the intrusion age. Like the QFP, this suggests emplacement occurred during, or quickly following, deposition of sediment at high levels in the crust.

The age of the second major phase of mafic rocks—biotite-rich trachyte dykes—is much more difficult to constrain. These intrude through the graphitic portion of the package and are thus younger than their deposition (maximum 1640 Ma). The trachyte also shows evidence of deformation; thus a pre- or syn-metamorphism age is likely.

The results from the alkaline rocks (syenite, glimmerite) are not easily interpreted. The U–Pb data across these samples are poor with significant discordance and generally scattered results. These rocks, as with the similarly disrupted felsic pegmatites, are commonly fluorite-bearing. Notwithstanding these difficulties, the data presented above suggests a *ca* 1616 Ma age for both the syenitic pegmatite and glimmerite. This age places these as coeval with the youngest (and compositionally variable) felsic phase, as well as some (if not all) mafic phases in the study area.

The various felsic pegmatites in the study area failed to yield any useful geochronological data owing to a lack of recovered zircons, and very imprecise analyses on those that were recovered. Field relationships with the 1641 Ma QFP are not clear, and it is probable that the pegmatites form part of the 1620–1610 Ma group. However, a younger age, such as peak of metamorphism, cannot be ruled out.

Bracketing the Milo beds

Attempts to directly date the various volcanic horizons within the Milo beds, in particular the apparent 'tuff' layers in the upper graphitic portions, were largely unsuccessful (zircons $<10\ \mu m$), despite high Zr abundance in many bulk rock analyses. However, a number of sedimentary samples (including marble) as well as the many other dates obtained during the study do allow for robust bracketing.

A presumed volcaniclastic rock (EX32127, this study) and GA sample 1925950 (Anderson *et al.*, 2017) suggest maximum depositional ages of *ca* 1660 Ma for the base units of the Milo beds. Other samples from this study from the mid (marble, 1651 Ma, EX096931) and upper sequence (schist in graphitic package, 1640 Ma, EX096917) have younger maximum depositional ages. These changes may represent a progression of time and sediment provenance through depositional history. The 1640 ± 11 Ma age from a muscovite schist at the top of the graphitic package (the highest part of the exposed Milo beds) is particularly interesting, as this age overlaps with the 1641 Ma QFP intrusion into the mid part of the sequence, which provides a minimum age for at least the lower Milo beds.

The stratigraphic position of the QFP intrusive unit in the study area approximately marks a shift in the sedimentary nature of the Milo beds. The lower sequence is dominated by quartzo-feldspathic volcaniclastic and clastic units, and the upper sequence is dominated by phyllosilicate and graphite rich metasiltstone and schists.

The maximum depositional age of 1640 ± 11 Ma for sample EX096917 suggests that at least part of the upper sequence postdates the QFP event, with rocks related to the QFP (perhaps extrusive equivalents) a likely source of the detrital zircons. With evidence of both a significant shift in sedimentary character and timing of deposition hinged around an intrusive event, it is possible that an unconformity or sedimentary hiatus exists between the upper and lower Milo beds, although the intense deformation fabrics would make identification of such in the field difficult. The timing of this event is similar to that of the Riversleigh Inversion identified in the Western Subprovince (Betts *et al.*, 2011); an unconformity in the Milo beds would be evidence for more widespread regional effects of this event.

The 1620–1610 Ma felsic units are intrusive and, along with an intruding mafic–ultramafic sill constrained as older than 1618 ± 10 Ma, place a lower bound on deposition in the central Tommy Creek area at *ca* 1620 Ma. This is in contrast to the interpretation of some previously reported samples with ages of *ca* 1615 Ma as being volcaniclastic (Carson *et al.*, 2011; Page & Sun, 1998). Field observations of the EX096916 (1616 ± 12 Ma) and GA/GSQ sample 1980491 (1615 ± 5 Ma) suggest they are the same rock type. However, the additional context of the intrusive 1641 Ma QFP and 1618 Ma gabbro in the study area and other ages from the Milo beds make the original interpretation of sample 1980491 as biotite psammite of possible volcanic origin difficult to justify. Instead, it is proposed that these samples represent thin sills, with subsequent metamorphism and deformation obscuring the contact relationships. Further work on the upper Milo beds, particularly to the south and east of the study area, may yield important information to constrain the upper age limit of deposition.

Overall, the data from this study bracket the deposition of the Milo beds between 1660 and 1620 Ma, with contemporaneous deposition of sediments and bimodal intrusive and extrusive units. Although perhaps not quite as young as previously suggested (Betts *et al.*, 2011; Carson *et al.*, 2011; Page & Sun, 1998), the ages presented here for the Milo beds still place it as the youngest pre-Isan Orogeny sedimentary sequence deposited in the Eastern Subprovince (Figure 7). Work by Griffin *et al.* (2006) showed the presence of detrital zircons in modern sediments taken within the Soldiers Cap Domain with a *ca* 1625 Ma age and highlighted a potential correlation with ages from the TCD. These zircons were interpreted to be mafic in origin and to be from the Toole Creek Volcanics. Although this age is not represented in the better-constrained samples of the Toole Creek Volcanics, they potentially indicate a correlation of mafic events in both domains. The lower Milo beds have a similar age to the youngest parts of the Soldiers Cap Group, Mount Albert Group and Kuridala Group, as well as the Mount Isa Group and lower McNamara Group of the Western Subprovince (Betts *et al.*, 2011; Foster & Austin, 2008).

A change in the sedimentary composition, and thus likely depositional environment, of the Milo beds from feldspathic metasediments and volcaniclastic rocks to organic rich shales could reflect the cessation of active extension at this time and may also relate to the Riversleigh Inversion event recorded in the Western Subprovince at *ca* 1640 Ma (Betts *et al.*, 2011). If this were the case, it would strengthen the interpretation of Gibson *et al.* (2016) on the stratigraphic position of the Isa Superbasin, although further consideration relating to some ages in the Loretta and River supersequences is required, and might place this event at *ca* 1647 Ma (Bradshaw *et al.*, 1999).

Metamorphism and hydrothermal events

The titanite U–Pb dataset provides some insight into the metamorphic and hydrothermal events. Most of the titanite data come from large single crystals, which may be vulnerable to outlier behaviour. This is highlighted in the results of EX32148 and EX096904, where the conventional crushed multigrain mineral separate data showed no evidence of the age produced from a single coarse (1–5 cm) crystal taken from same drill core.

The *ca* 1525 Ma age found in three of the seven titanite samples is well represented in other geochronological studies of the Eastern Subprovince, such as titanites from Mary Kathleen (Spandler *et al.*, 2016) and some of the William Batholith intrusive suite (Betts *et al.*, 2011; Murphy *et al.*, 2017). This age is postulated to be a significant time for hydrothermal alteration across the region (Oliver *et al.*, 2008), so it is not surprising to see it represented at Tommy Creek.

The two ages (*ca* 1560 Ma and *ca* 1525 Ma) obtained from the syenite samples point to some complexity in the ages preserved by the titanites. The multigrain 1560 Ma result is likely a more robust age representing a high proportion of titanite within these rocks, with some titanite modification at 1525 Ma possible. Neither of these ages matches the zircon ages, suggesting that the titanite is not magmatic in origin or that any such titanite has been comprehensively reset. The titanite from the metagabbro also likely represents a metamorphic event, with the *ca* 1600 Ma age consistent with the work of Pourteau *et al.* (2018).

Comparison with previous work

This study has significantly expanded the breadth of ages to constrain the evolution of the TCD. The previous work focused primarily on the felsic rocks, and the stratigraphic framework hinged on the interpretation of the nature of these samples. These earlier works have only recognised one or two felsic phases (the *ca* 1650 Ma Tommy Creek Microgranite and volcaniclastic rocks). However, the results

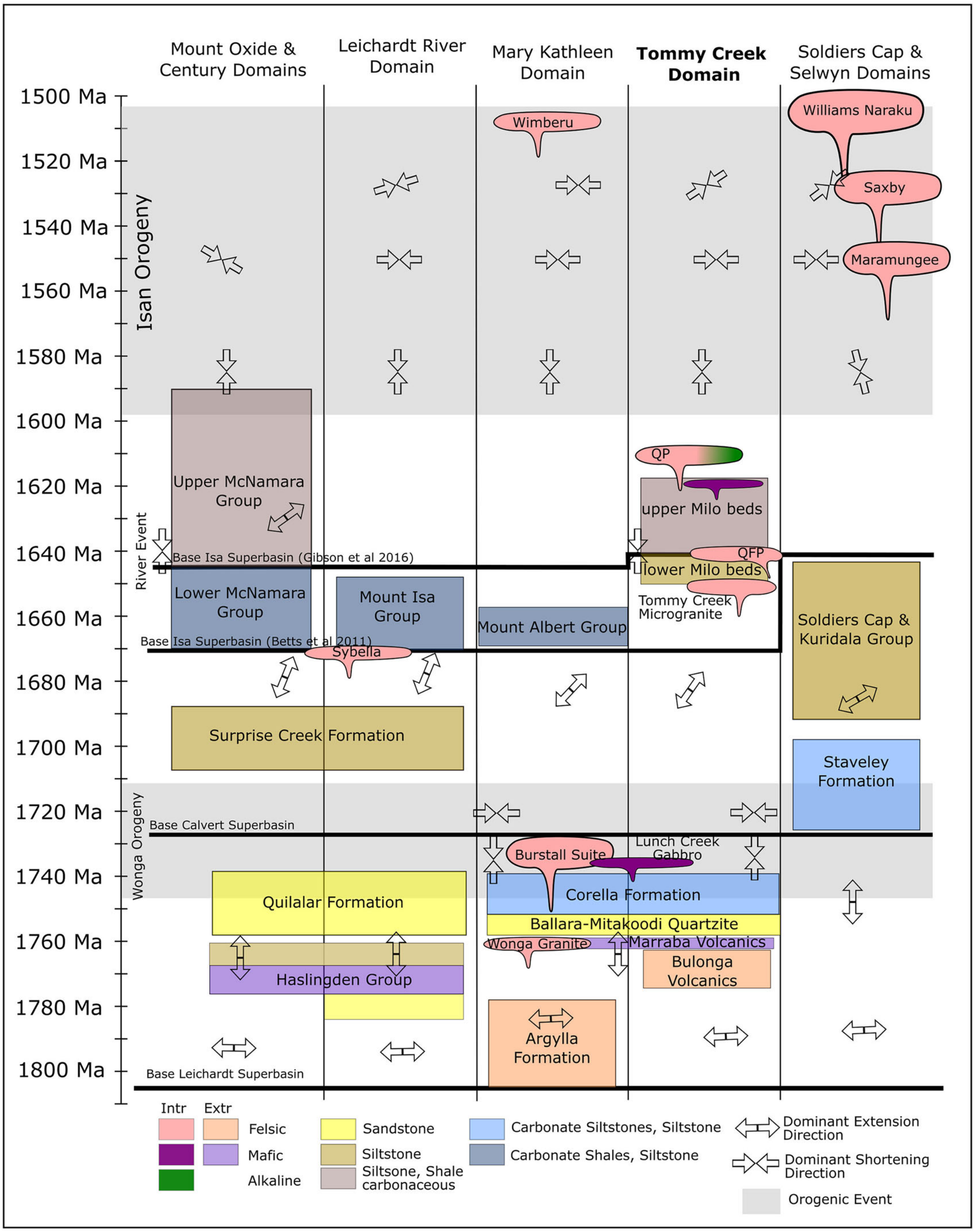

Figure 7. Simplified time–space plot of the tectonostratigraphic framework of the Mount Isa Inlier, including the Tommy Creek Domain. Modified from Betts *et al.* (2011) and Murphy *et al.* (2017) with interpretations from this study, the Wonga Orogeny from Spence *et al.* (2022) and the Isa Superbasin interpretation of Gibson *et al.* (2016).

of this study suggest at least four phases of felsic rocks, both volcanic (lower Milo beds) and intrusive (Tommy Creek Microgranite, 1641 Ma porphyritic sills, 1620–1610 Ma sills, dykes and stocks), including ages not previously recognised in the Eastern Subprovince. The earlier volcaniclastic interpretations depended largely on field observations such as relict fiamme (Hill *et al.*, 1992), which were made separately to the geochronology samples in other locations (Page & Sun, 1998). This study suggests that the volcaniclastic rocks are part of the lower Milo beds (*ca* 1660 Ma), and that the previous geochronology samples are from the 1620–1610 Ma intrusive suite. Given the scale at which the previous work was performed, and the complication of complex deformation and metamorphism, such generalisation of units is understandable. A more integrated approach of mapping and geochronology has allowed a more robust and nuanced interpretation of the geology of the TCD and highlights the need to carefully consider scale when interpreting geochronological datasets, particularly in complex terranes.

Tectonic setting

The sedimentary and intrusive history of the TCD is consistent with a rifting environment; however contemporaneous deposition and emplacement of bimodal magmatism at high crustal levels at *ca* 1640–1620 Ma (Figure 5) suggest that active extension may have continued through to the early stages of the Isan Orogeny (*ca* 1605 Ma; Pourteau *et al.*, 2018). The multimodal intrusions identified in this study at *ca* 1615 Ma may be part of this switch to compressional tectonics, but they may also be indicative of other crustal processes such as crustal thinning and/or delamination and mafic underplating associated with extension (Chen *et al.*, 2021; Cheng *et al.*, 2013).

Although the geodynamic history of the Mount Isa Province is broadly described as extensional between the Barramundi Orogeny (*ca* 1900–1870 Ma) and the Isan Orogeny (*ca* 1600–1500 Ma), some workers have recognised sedimentary hiatuses and basin inversion events punctuating the depositional record (Betts *et al.*, 2011; Gibson *et al.*, 2016). Spence *et al.* (2022) reinterpreted evidence of extensional decollement (Holcombe *et al.*, 1991; Oliver *et al.*, 1991) with new field data to propose the Wonga Orogeny, which points towards significant contractional deformation at 1750–1710 Ma marking the boundary between rifting cycles of the Leichardt and Calvert superbasins. The high-level felsic intrusions and switch in sedimentary character of the Milo beds (*ca* 1640 Ma) are coincident with the Riversleigh Inversion identified in the Lawn Hill Platform (Betts *et al.*, 2011; Bradshaw *et al.*, 2000) in the Western Subprovince, as well as an early foliation development in the Snake Creek Anticline in the Soldiers Cap Domain (Rubenach *et al.*, 2008). This may point to a widespread but transient contractional event at this time, and that the evolution of the Mount Isa Inlier is more correctly characterised by oscillatory extensional–contractional tectonic environment, rather than a continuous series of rift-sag phases.

Conclusions

A total of 23 new ages from sedimentary and igneous lithologies of the central TCD allow refinement of the geochronological framework of the Mount Isa Province. The Milo beds (1660–1620 Ma) are confirmed as the youngest stratigraphic unit in the Eastern Subprovince, with the upper Milo beds comparable with the upper McNamara Group of the Century and Mount Oxide domains of the Western Succession, whereas the lower Milo beds correlate with the lower McNamara and Mount Isa groups in the west, and the Soldiers Cap, Mount Albert and Kuridala groups in the east. Previously reported ages of *ca* 1615 Ma are reinterpreted to represent intrusive units. Detrital zircon and intrusive ages in the Milo beds show contemporaneous intrusion of rhyodacite sills coincident with a switch from feldspathic and volcaniclastic metasediments to carbon rich and clastic starved sediments at *ca* 1640 Ma. This suggests a change from an active extensional setting, and the correlation with the Riversleigh Inversion event recorded in the Lawn Hill Platform suggests a brief regional contractional event may have occurred. An expanded and more nuanced framework for the TCD includes a suite of felsic, mafic and alkaline rocks with ages (1640 Ma, 1620–1610 Ma) not previously recognised as prominent in the Mount Isa Province, occurring immediately before, or in the early stages of, the Isan Orogeny.

The accessibility of laser ablation geochronology affords a shift in sampling attitude to allow for a higher-volume approach, including unconventional target lithologies (such as mafic or carbonate dominant). Combined with fast turnaround times, this allows for the field mapping and geochronology to be integrated in an iterative approach, and results in efficient identification of complexities and distinction between similar units in a field area. This has been the case in this study from the TCD, with new ages presented here identifying previously unrecognised intrusive phases, leading to a new framework for a complicated terrane within the Eastern Subprovince of the Mount Isa Province.

Acknowledgements

The authors thank the technical assistance from James Cook University colleagues Yi Hu and Shane Askew of the Advanced Analytical Centre as well as Huiqing Huang. Valuable feedback on the manuscript from anonymous reviewers is very much appreciated.

Disclosure statement

No potential conflict of interest was reported by the author(s).

Funding

The project has been financially supported by Mount Isa Mines Resource Development Pty Limited, with whom A. Brown was employed for the duration of the project.

ORCID

A. Brown http://orcid.org/0000-0001-7535-9200
C. Spandler http://orcid.org/0000-0003-2310-0517
T. G. Blenkinsop http://orcid.org/0000-0001-9684-0749

Data availability statement

Data supporting the findings of this paper can be accessed at James Cook University at https://doi.org/10.25903/q81t-7t34

References

Abu Sharib, A. S. A. A., & Sanislav, I. V. (2013). Polymetamorphism accompanied switching in horizontal shortening during Isan

Orogeny: Example from the Eastern Fold Belt, Mount Isa Inlier, Australia. *Tectonophysics*, *587*, 146–167. https://doi.org/10.1016/j.tecto.2012.06.051

Anderson, J. R., Fraser, G. L., McLennan, S. M., & Lewis, C. J. (2017). *A U–Pb geochronology compilation for northern Australia: Version 1, November 2017*. Geoscience Australia Record 2017/22.

Bea, F., Bortnikov, N., Cambeses, A., Chakraborty, S., Molina, J. F., Montero, P., Morales, I., Silantiev, S., & Zinger, T. (2022). Zircon crystallization in low-Zr mafic magmas: Possible or impossible? *Chemical Geology*, *602*, 120898. https://doi.org/10.1016/j.chemgeo.2022.120898

Betts, P. G., Armit, R. J., Hutton, L. J., Withnall, I. W., & Donchak, P. J. T. (2011). Mount Isa Inlier Geodynamic Synthesis. In *North West Queensland Mineral and Energy Province Report*. Geological Survey Queensland.

Betts, P. G., Giles, D., Mark, G., Lister, G. S., Goleby, B. R., & Aillères, L. (2006). Synthesis of the proterozoic evolution of the Mt Isa Inlier. *Australian Journal of Earth Sciences*, *53*(1), 187–211. https://doi.org/10.1080/08120090500434625

Black, L. P., Kamo, S. L., Allen, C. M., Aleinikoff, J. N., Davis, D. W., Korsch, R. J., & Foudoulis, C. (2003). TEMORA 1: A new zircon standard for Phanerozoic U–Pb geochronology. *Chemical Geology*, *200*(1-2), 155–170. https://doi.org/10.1016/S0009-2541(03)00165-7

Blake, D. H. (1987). *Geology of the Mount Isa Inlier and environs, Queensland and Northern Territory*. Australian Government Publishing Service.

Blake, D. H. & Stewart, A. J. (Eds.) (1992). *Detailed studies of the Mount Isa Inlier*. Bureau of Mineral Resources. Bulletin 243.

Bradshaw, B. E., Lindsay, J. F., Krassay, A. A., & Wells, A. T. (2000). Attenuated basin-margin sequence stratigraphy of the Palaeoproterozoic Calvert and Isa Superbasins: The Fickling Group, southern Murphy Inlier, Queensland. *Australian Journal of Earth Sciences*, *47*(3), 599–623. https://doi.org/10.1046/j.1440-0952.2000.00794.x

Bradshaw, B. E., Scott, D. L., & Southgate, P. N. (1999). *Integrated basin analysis of the Isa Superbasin using seismic, well log and geopotential data: An evaluation of the economic potential of the Northern Lawn Hill Platform*. Geoscience Australia Record 1999/019.

Carson, C. J., Hutton, L. J., Withnall, I. W., Perkins, W. G., Donchak, P. J. T., Parsons, A., Blake, P. R., Sweet, I. P., Neumann, N. L., & Lambeck, A., (2011). *Summary of results: Joint GSQ-GA NGA geochronology p. oject, Mount Isa region, 2009–2010*. Queensland Geological Record 2011/03.

Carter, E. K., & Öpik, A. A. (1961). *Lawn Hill, 4-mile geological series: Sheet E/54-9, Australian National Grid*. Bureau of Mineral Resources.

Chen, G., Liu, R., Deng, T., & Wang, L. (2021). Bimodal magmatism produced by delamination: Geochemical evidence from late Palaeozoic volcanic rocks from the Yili Block, Western Tianshan, Northwestern China. *Geological Magazine*, *158*(6), 1059–1073. https://doi.org/10.1017/S0016756820001090

Cheng, Y., Mao, J., & Spandler, C. (2013). Petrogenesis and geodynamic implications of the Gejiu igneous complex in the western Cathaysia block, South China. *Lithos*, *175-176*, 213–229. https://doi.org/10.1016/j.lithos.2013.04.002

Cherniak, D. J. (1993). Lead diffusion in titanite and preliminary results on the effects of radiation damage on Pb transport. *Chemical Geology*, *110*(1-3), 177–194. https://doi.org/10.1016/0009-2541(93)90253-F

Derrick, G. M. (1980a). *Marraba Queensland 1:100000 Geological Map Commentary*. Bureau of Mineral Resources.

Derrick, G. M. (1980b). *Australia 1:100 000 geological series. Sheet 6956 [Erl.]: Marraba: Queensland Commentary*. Australian Government Publishing Service.

Etheridge, M. A., Rutland, R. W. R., & Wyborn, L. A. I. (1987). Orogenesis and tectonic process in the early to middle Proterozoic of northern Australia. In A. Kröner (Ed.), *Proterozoic Lithospheric Evolution* (pp. 131–147). American Geophysical Union (AGU). https://doi.org/10.1029/GD017p0131

Foster, D. R. W., & Austin, J. (2008). The 1800–1610Ma stratigraphic and magmatic history of the Eastern Succession, Mount Isa Inlier, and correlations with adjacent Paleoproterozoic terranes. *Precambrian Research*, *163*(1-2), 7–30. https://doi.org/10.1016/j.precamres.2007.08.010

Foster, D. R. W., & Rubenach, M. J. (2006). Isograd pattern and regional low-pressure, high-temperature metamorphism of pelitic, mafic and calc-silicate rocks along an east – west section through the Mt Isa Inlier. *Australian Journal of Earth Sciences*, *53*(1), 167–186. https://doi.org/10.1080/08120090500434617

Frost, B. R., Chamberlain, K., & Schumacher, J. (2001). Sphene (titanite): Phase relations and role as a geochronometer. *Chemical Geology*, *172*(1-2), 131–148. https://doi.org/10.1016/S0009-2541(00)00240-0

Geological Survey of Queensland, Young, L. J., Lane, R. P., Withnall, I. W., Parsons, A., Pascoe, G. S., Turner, S. M. (2015). *Marraba, Queensland* [Map]. Geoscience Australia.

Geological Survey of Queensland (2011). *North-West Queensland Mineral and Energy Province report*. Geological Survey of Queensland. https://trove.nla.gov.au/version/93308448

Gibson, G. M., Champion, D. C., Withnall, I. W., Neumann, N. L., & Hutton, L. J. (2018). Assembly and breakup of the Nuna supercontinent: Geodynamic constraints from 1800 to 1600 Ma sedimentary basins and basaltic magmatism in northern Australia. *Precambrian Research*, *313*, 148–169. https://doi.org/10.1016/j.precamres.2018.05.013

Gibson, G. M., Meixner, A. J., Withnall, I. W., Korsch, R. J., Hutton, L. J., Jones, L. E. A., Holzschuh, J., Costelloe, R. D., Henson, P. A., & Saygin, E. (2016). Basin architecture and evolution in the Mount Isa mineral province, northern Australia: Constraints from deep seismic reflection profiling and implications for ore genesis. *Ore Geology Reviews*, *76*, 414–441. https://doi.org/10.1016/j.oregeorev.2015.07.013

Giles, D., Betts, P., & Lister, G. (2002). Far-field continental backarc setting for the 1.80–1.67 Ga basins of northeastern Australia. *Geology*, *30*(9), 823–826. https://doi.org/10.1130/0091-7613(2002)030<0823:FFCBSF>2.0.CO;2

Giles, D., & Nutman, A. P. (2002). SHRIMP U–Pb monazite dating of 1600–1580 Ma amphibolite facies metamorphism in the southeastern Mt Isa Block, Australia. *Australian Journal of Earth Sciences*, *49*(3), 455–465. https://doi.org/10.1046/j.1440-0952.2002.00931.x

Griffin, W. L., Belousova, E. A., Walters, S. G., & O'Reilly, S. Y. (2006). Archaean and Proterozoic crustal evolution in the Eastern Succession of the Mt Isa district, Australia: U–Pb and Hf-isotope studies of detrital zircons. *Australian Journal of Earth Sciences*, *53*(1), 125–149. https://doi.org/10.1080/08120090500434591

Hand, M., McLaren, S., & Rubatto, D. (2002). The scale of the thermal problem in the Mount Isa Inlier. *Geological Society of Australia Abstracts*, *67*, 173.

Harrison, T., Baldwin, S., Caffee, M., Gehrels, G., Schoene, B., Shuster, D., & Singer, B. (2015). *It's about time: Opportunities and challenges for US geochronology*. Institute of Geophysics and Planetary Physics Publication 6539, University of California, Los Angeles.

Hill, E. J. (1987). *Structural Geology of the Tommy Creek Area, Mount Isa Inlier, NW Queensland*. Bureau of Mineral Resources, Record 1987/20/.

Hill, E. J., Loosveld, R. J. H., & Page, R. W. (1992). Structure and Geochronology of the Tommy Creek Block, Mount Isa Inlier. In D. H. Blake & A. J. Stewart (Eds.), *Detailed studies of the Mount Isa Inlier* (pp. 329–348). Bureau of Mineral Resources. Bulletin 243.

Holcombe, R. J., Pearson, P. J., & Oliver, N. H. S. (1991). Geometry of a Middle Proterozoic extensional décollement in northeastern Australia. *Tectonophysics*, *191*(3-4), 255–274. https://doi.org/10.1016/0040-1951(91)90061-V

Jackson, S. E., Pearson, N. J., Griffin, W. L., & Belousova, E. A. (2004). The application of laser ablation-inductively coupled plasma-mass spectrometry to in situ U–Pb zircon geochronology. *Chemical Geology*, *211*(1-2), 47–69. https://doi.org/10.1016/j.chemgeo.2004.06.017

Jackson, M. J., Scott, D. L., & Rawlings, D. J. (2000). Stratigraphic framework for the Leichhardt and Calvert Superbasins: Review and correlations of the pre- 1700 Ma successions between Mt Isa and

McArthur River. *Australian Journal of Earth Sciences*, *47*(3), 381–403. https://doi.org/10.1046/j.1440-0952.2000.00789.x

Jell, P. A. (Ed.). (2013). *Geology of Queensland*. Geological Survey of Queensland.

Lally, J. (1997). *The structural history of the central Eastern Fold Belt, Mount Isa Inlier, Northwest Queensland, Australia* [unpublished PhD Thesis]. James Cook University.

Loosveld, R. J. H. (1989). The intra-cratonic evolution of the central eastern Mount Isa Inlier, northwest Queensland, Australia. *Precambrian Research*, *44*(3-4), 243–276. https://doi.org/10.1016/0301-9268(89)90047-8

Loosveld, R. J. H., & Etheridge, M. A. (1990). A model for low-pressure facies metamorphism during crustal thickening. *Journal of Metamorphic Geology*, *8*(3), 257–267. https://doi.org/10.1111/j.1525-1314.1990.tb00472.x

Ludwig, K. (2012). *ISOPLOT | BGC*. Berkeley Geochronology Center. https://www.bgc.org/isoplot

McLaren, S., Sandiford, M., & Hand, M. (1999). High radiogenic heat–producing granites and metamorphism—An example from the western Mount Isa inlier, Australia. *Geology*, *27*(8), 679–682. https://doi.org/10.1130/0091-7613(1999)027<0679:HRHPGA>2.3.CO;2

Murphy, T., Hinman, M., Donohue, J., Pirlo, M., Valenta, R., Jones, M., & Pratt, A. (2017). *Deep Mining Queensland Prospectivity Analysis in the Southern Cloncurry Belt*. Commissioned Industry Study No. CR102015, Geological Survey of Queensland.

Oliver, N. H. S., Butera, K., Rubenach, M. J., Marshall, L., Cleverley, J., Mark, G., Tullemans, F., & Esser, D. (2008). The protracted hydrothermal evolution of the Mount Isa Eastern Succession: A review and tectonic implications. *Precambrian Research*, *163*(1-2), 108–130. https://doi.org/10.1016/j.precamres.2007.08.019

Oliver, N. H. S., Holcombe, R. J., Hill, E. J., & Pearson, P. J. (1991). Tectono-metamorphic evolution of the Mary Kathleen fold belt, northwest Queensland: A reflection of mantle plume processes? *Australian Journal of Earth Sciences*, *38*(4), 425–455. https://doi.org/10.1080/08120099108727982

Paces, J. B., & Miller, J. D. Jr, (1993). Precise U–Pb ages of Duluth Complex and related mafic intrusions, northeastern Minnesota: Geochronological insights to physical, petrogenetic, paleomagnetic, and tectonomagmatic processes associated with the 1.1 Ga Midcontinent Rift System. *Journal of Geophysical Research: Solid Earth*, *98*(B8), 13997–14013. https://doi.org/10.1029/93JB01159

Page, R. W. (1983). Timing of superposed volcanism in the Proterozoic Mount Isa Inlier, Australia. *Precambrian Research*, *21*(3-4), 223–245. https://doi.org/10.1016/0301-9268(83)90042-6

Page, R. W., & Bell, T. H. (1986). Isotopic and structural responses of granite to successive deformation and metamorphism. *Journal of Geology*, *94*(3), 365–379. https://doi.org/10.1086/629035

Page, R. W., & Sun, S. (1998). Aspects of geochronology and crustal evolution in the Eastern Fold Belt, Mt Isa Inlier. *Australian Journal of Earth Sciences*, *45*(3), 343–361. https://doi.org/10.1080/08120099808728396

Paton, C., Hellstrom, J., Paul, B., Woodhead, J., & Hergt, J. (2011). Iolite: Freeware for the visualisation and processing of mass spectrometric data. *Journal of Analytical Atomic Spectrometry*, *26*(12), 2508–2518. https://doi.org/10.1039/c1ja10172b

Pourteau, A., Smit, M. A., Li, Z-X., Collins, W. J., Nordsvan, A. R., Volante, S., & Li, J. (2018). 1.6 Ga crustal thickening along the final Nuna suture. *Geology*, *46*(11), 959–962. https://doi.org/10.1130/G45198.1

Rubenach, M. J. (1992). Proterozoic low-pressure/high-temperature metamorphism and an anticlockwise P–T–t path for the Hazeldene area, Mount Isa Inlier, Queensland, Australia. *Journal of Metamorphic Geology*, *10*(3), 333–346. https://doi.org/10.1111/j.1525-1314.1992.tb00088.x

Rubenach, M. J., & Barker, A. J. (1998). Metamorphic and metasomatic evolution of the Snake Creek Anticline, Eastern Succession, Mt Isa Inlier. *Australian Journal of Earth Sciences*, *45*(3), 363–372. https://doi.org/10.1080/08120099808728397

Rubenach, M. J., Foster, D., Evins, P., Blake, K., & Fanning, C. (2008). Age constraints on the tectonothermal evolution of the Selwyn Zone, Eastern Fold Belt, Mount Isa Inlier. *Precambrian Research*, *163*(1-2), 81–107. https://doi.org/10.1016/j.precamres.2007.08.014

Sandiford, M., Eraser, G., Arnold, J., Foden, J., & Farrow, T. (1995). Some causes and consequences of high-temperature, low-pressure metamorphism in the eastern Mt Lofty Ranges, South Australia. *Australian Journal of Earth Sciences*, *42*(3), 233–240. https://doi.org/10.1080/08120099508728197

Sandiford, M., Hand, M., & McLaren, S. (1998). High geothermal gradient metamorphism during thermal subsidence. *Earth and Planetary Science Letters*, *163*(1-4), 149–165. https://doi.org/10.1016/S0012-821X(98)00183-6

Southgate, P. N., Bradshaw, B. E., Domagala, J., Jackson, M. J., Idnurm, M., Krassay, A. A., Page, R. W., Sami, T. T., Scott, D. L., Lindsay, J. F., McConachie, B. A., & Tarlowski, C. (2000). Chronostratigraphic basin framework for Palaeoproterozoic rocks (1730–1575 Ma) in northern Australia and implications for base-metal mineralisation. *Australian Journal of Earth Sciences*, *47*(3), 461–483. https://doi.org/10.1046/j.1440-0952.2000.00787.x

Spandler, C., Hammerli, J., Sha, P., Hilbert-Wolf, H., Hu, Y., Roberts, E., & Schmitz, M. (2016). MKED1: A new titanite standard for *in situ* analysis of Sm–Nd isotopes and U–Pb geochronology. *Chemical Geology*, *425*, 110–126. https://doi.org/10.1016/j.chemgeo.2016.01.002

Spence, J. S., Sanislav, I. V., & Dirks, P. H. G. M. (2022). Evidence for a 1750–1710 Ma orogenic event, the Wonga Orogeny, in the Mount Isa Inlier, Australia: Implications for the tectonic evolution of the North Australian Craton and Nuna Supercontinent. *Precambrian Research*, *369*, 106510. https://doi.org/10.1016/j.precamres.2021.106510

Spencer, C. J., Kirkland, C. L., & Taylor, R. J. M. (2016). Strategies towards statistically robust interpretations of in situ U–Pb zircon geochronology. *Geoscience Frontiers*, *7*(4), 581–589. https://doi.org/10.1016/j.gsf.2015.11.006

Stacey, J. S., & Kramers, J. D. (1975). Approximation of terrestrial lead isotope evolution by a two-stage model. *Earth and Planetary Science Letters*, *26*(2), 207–221. https://doi.org/10.1016/0012-821X(75)90088-6

Todd, C. N., Roberts, E. M., Knutsen, E. M., Rozefelds, A. C., Huang, H-Q., & Spandler, C. (2019). Refined age and geological context of two of Australia's most important Jurassic vertebrate taxa (*Rhoetosaurus brownei* and *Siderops kehli*), Queensland. *Gondwana Research*, *76*, 19–25. https://doi.org/10.1016/j.gr.2019.05.008

Wiedenbeck, M., Allé, P., Corfu, F., Griffin, W I., Meier, M., Oberli, F., Quadt, A V., Roddick, J. C., & Spiegel, W. (1995). Three Natural Zircon Standards for U–Th–Pb, Lu–Hf, Trace Element and Ree Analyses. *Geostandards and Geoanalytical Research*, *19*(1), 1–23. https://doi.org/10.1111/j.1751-908X.1995.tb00147.x

Wilson, I. H. (1978). Volcanism on a Proterozoic continental margin in northwestern Queensland. *Precambrian Research*, *7*(3), 205–235. https://doi.org/10.1016/0301-9268(78)90039-6